

Review

Carbon Nanotube Field-Effect Transistor-Based Chemical and Biological Sensors

Xuesong Yao ^{1,†}, Yalei Zhang ^{1,†}, Wanlin Jin ², Youfan Hu ^{2,*} and Yue Cui ^{1,*}

¹ School of Materials Science and Engineering, Peking University, Beijing 100871, China; 1801214055@pku.edu.cn (X.Y.); zhangyalei@pku.edu.cn (Y.Z.)

² Key Laboratory for the Physics and Chemistry of Nanodevices, Center for Carbon-Based Electronics, Frontiers Science Center for Nano-Optoelectronics, and Department of Electronics, Peking University, Beijing 100871, China; 1801213549@pku.edu.cn

* Correspondence: youfanhu@pku.edu.cn (Y.H.); ycui@pku.edu.cn (Y.C.)

† These authors contribute equally to this work.

Abstract: Chemical and biological sensors have attracted great interest due to their importance in applications of healthcare, food quality monitoring, environmental monitoring, etc. Carbon nanotube (CNT)-based field-effect transistors (FETs) are novel sensing device configurations and are very promising for their potential to drive many technological advancements in this field due to the extraordinary electrical properties of CNTs. This review focuses on the implementation of CNT-based FETs (CNTFETs) in chemical and biological sensors. It begins with the introduction of properties, and surface functionalization of CNTs for sensing. Then, configurations and sensing mechanisms for CNT FETs are introduced. Next, recent progresses of CNTFET-based chemical sensors, and biological sensors are summarized. Finally, we end the review with an overview about the current application status and the remaining challenges for the CNTFET-based chemical and biological sensors.

Keywords: carbon nanotube; field-effect transistors; sensors; chemical; biological



Citation: Yao, X.; Zhang, Y.; Jin, W.; Hu, Y.; Cui, Y. Carbon Nanotube Field-Effect Transistor-Based Chemical and Biological Sensors. *Sensors* **2021**, *21*, 995. <https://doi.org/10.3390/s21030995>

Academic Editor: Benoît Piro
Received: 31 December 2020
Accepted: 26 January 2021
Published: 2 February 2021

Publisher's Note: MDPI stays neutral with regard to jurisdictional claims in published maps and institutional affiliations.



Copyright: © 2021 by the authors. Licensee MDPI, Basel, Switzerland. This article is an open access article distributed under the terms and conditions of the Creative Commons Attribution (CC BY) license (<https://creativecommons.org/licenses/by/4.0/>).

1. Introduction

Chemical and biological sensors have attracted great attention recently, and have a wide range of applications in healthcare, environmental monitoring, food quality, and defense. These sensors can respond to specific chemical or biological compounds and convert this information into electrical signals. Many materials have been studied as the sensitive materials in the chemical/biological sensors, such as SnO₂ [1,2], ZnO₂ [3], Ag [4], and graphene [5]. Generally speaking, the ideal material in chemical and biological sensors should have a high chemical reactivity, a large surface to volume ratio or an easy fabrication at low cost.

Carbon nanotubes (CNTs) are seamless nanotubes made of single or multiple layers of graphene sheets rolled around a central axis with the advantages of being lightweight and having a perfect hexagonal connection structure. The unique electronic transport properties of CNTs make them potentially useful in nanodevices [6,7]. For example, CNTs are atomically thin in order to provide ideal electrostatic control over the channel, which is quite important when the device is scaled down. This unique atomically thin structure of CNTs also gives them many advantages when serving as the sensitive materials in sensors, and the electrical performance superiority of CNT-based field effect transistors (CNTFETs) has been extended in various chemical and biological sensors. Compared with other detecting technologies, CNTFET-based sensors have the advantages of high sensitivity, high selectivity, simple operation, low operating temperature, fast response speed, short recovery time, label-free detection, and good stability. Referring to the detection capability of various substances and the exceptional performance, CNTFETs are expected to play an increasing role in the field of sensing. In this review, the properties of CNTs, configurations

and sensing mechanisms based on CNTFETs, recent progresses of the implementation of CNTFETs in chemical sensors and biological sensors, and the perspective of this technology are introduced.

2. Surface Functionalization of CNTs for Sensing

2.1. Covalent Modification

Covalent modification mainly involves chemical destruction of C-C bonds of the CNTs ports or sidewalls to generate more polar carboxyl groups or hydroxyl groups on the surfaces. Then, various functional groups can be introduced on the CNT surfaces to further attach the derivative reaction of the target product to the CNTs—for example, chemical groups, fluorescently labeled molecules, DNA, anticancer drugs, etc. The oxidants used for covalently modification include nitric acid, mixed acid (concentrated sulfuric acid/nitric acid), neutral hydrogen peroxide, and sodium hydroxide, as shown in Figure 1. The disadvantage of covalent modification is that it may destroy the integrity of CNTs, which will affect its mechanical and electrical properties to some extent.

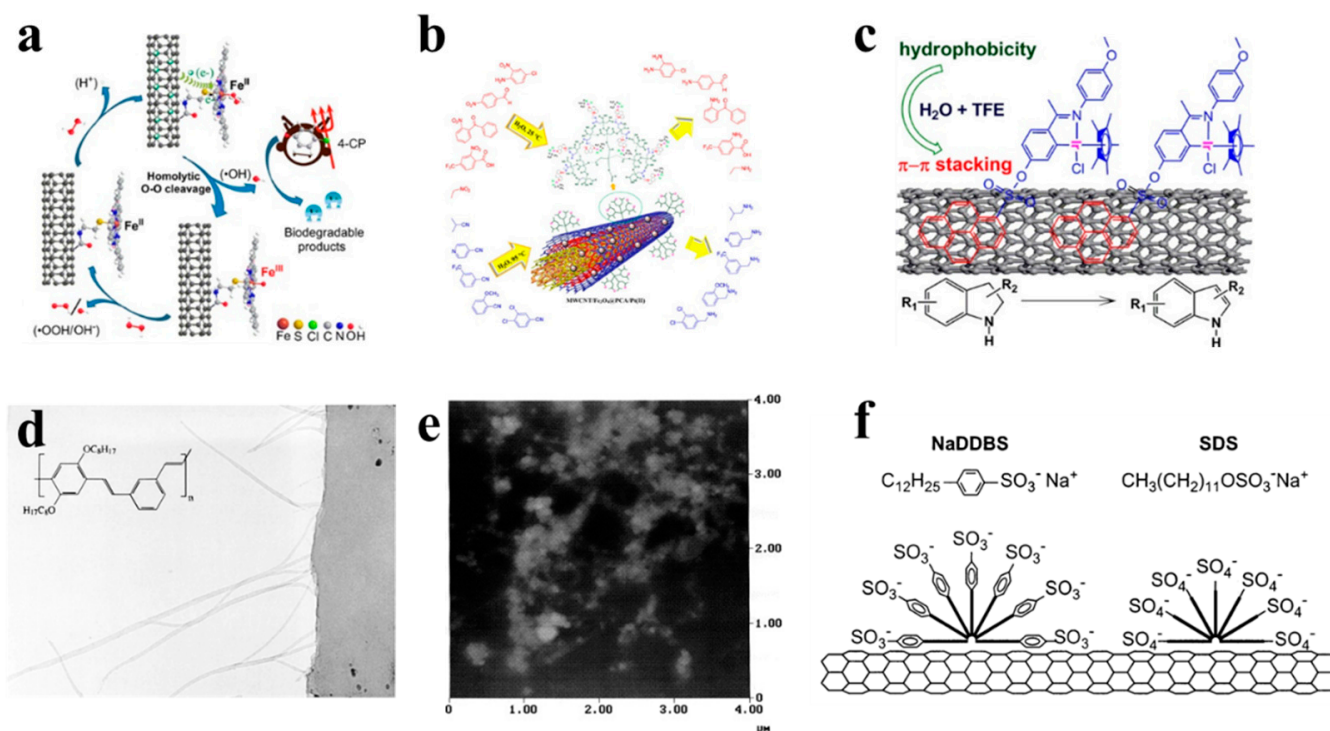


Figure 1. Surface functionalization of carbon nanotubes (CNTs). (a) The introduction of the -COOH group to the surface of the CNT [8]. (b) The introduction of -COOH on the surface of CNTs by the oxidation reaction [9]. (c) A metal iridium complex catalyst was coated on the surface of CNTs through non-covalent bond accumulation [10]. (d) TEM image which shows the nominal chemical structure of the polymer backbone [11]. (e) The atomic force microscopy image of the waxy corn amylopectin-single-walled CNT (SWCNT) film [12]. (f) Schematic representation of surfactants adsorb onto the CNT surfaces [13].

As shown in Figure 1a, Ni et al. [8] introduced the -COOH derivative group on the surface of the CNT by the oxidation reaction, and two different ligands are introduced on the CNT surface, including aminopyridine and aminoethyl mercaptan curing catalyst iron phthalocyanine (VE-H). As shown in Figure 1b, Rezaie et al. [9] also introduced -COOH to the surface of CNTs by oxidation reaction, then formed a dendrimer with poly(citric acid), and then attached a divalent platinum metal catalyst to the surface of CNTs. Finally, a magnetic catalyst was obtained. The catalyst can selectively reduce nitro and nitrile.

2.2. Non-Covalent Modification

Non-covalent modification means that covalent chemical bonds are not introduced for modification on the surface of CNTs, but are achieved through non-covalent bonding, including physical adsorption and surface coating. The non-covalent modification is mainly formed by the hybridization of carbon atoms sp^2 in the graphene structure of the sidewall to form highly delocalized electrons and electrons of other compounds to generate non-covalent bonds. The non-covalent interactions include dispersion forces, hydrogen bonds, dipole-dipole forces, π - π stacking effects, and hydrophobic effects. Carbon atoms in CNTs are all SP^2 hybrids, forming highly delocalized electrons, which can be modified with other π electron-rich compounds through π - π stacking. The non-covalently modified CNTs are structurally complete and can retain their original properties. The molecules for the non-covalent modification mainly include the surfactants, the molecules containing aromatic groups, and the polymers. For biological sensors, the non-covalent modification of the CNTs can not only improve their water solubility in biological systems, but also can avoid the non-specific adsorption of the biomolecules.

As shown in Figure 1c, Liu et al. [10] coated the metal iridium complex catalyst on the surface of CNTs through non-covalent bond accumulation, and the coating efficiency reached over 94%. The metal iridium complex catalyst is coated on CNT to make the catalytic dehydrogenation reaction of indole from organics such as methanol, ethanol, tetrahydrofuran, trifluoroethanol, etc. The transfer of solvents to water makes this organic reaction more environmentally friendly. The surfactant contains two parts, which are the lipophilic end and the hydrophilic end. When they are adsorbed on the surface by the CNTs, the charge repulsion disperses them. Under thermodynamics, water-soluble polymers such as sodium polystyrene sulfonate entangle CNTs, thereby exerting the role of surfactants and making them amphiphilic [14]. As shown in Figure 1d, Dalton et al. [11] used conjugated poly-phenylene vinylene to surface-coat the CNTs, and found that the CNTs were evenly dispersed in the polymer matrix. As shown in Figure 1e, Stobinski et al. [12] modified CNTs with sodium lauryl sulfate and dispersed them by ultrasound. It was found that increasing the ultrasonic time or decreasing the concentration of the suspension can obtain CNT solutions with better dispersion properties. As shown in Figure 1f, coating CNTs with sodium benzoate and sodium dodecyl benzenesulfonate can also increase their water solubility [13].

3. Configuration and Sensing Mechanism

3.1. General CNTFETs

CNTFETs have a variety of structures [15], but share similar characteristics: the conductive channel, source and drain electrodes, a gate electrode on the top or bottom of the channel, and a dielectric layer between the channel and the gate to separate the gate electrode from the CNTs. The operating principles of these CNTFETs are similar: the gate electrode uses a vertical electric field to control the amount of charge in the channel; the horizontal electric field between the source and drain electrodes provides driving force, and a current is made to flow from one electrode through the CNT to the other electrode [16].

Figure 2a shows a typical configuration of a CNTFET for sensing purpose. In general, the transport of carriers in a CNTFET can be attributed to four states, which are independent of the device structure [17]. The classification of these states depends on the comparison of the CNT length and the mean free path length of the CNT, and the type of contact between the CNT and the source and drain [18]. For example, an ohmic contact ballistic CNTFET means that carriers are injected into the CNTs from the source and the drain through an ohmic contact, and the carrier transport process in the CNT is not subjected to any scattering. In contrast, Schottky-type diffused CNTFETs mean that the carrier injection is affected by a Schottky barrier derived from the heterojunction of the electrode and the CNT, and the carriers are constantly scattered during transmission in the conductive channel. There are two kinds of carriers: holes and electrons. If the type of carriers is mainly electrons, then the FET is an n-type transistor; on the other hand, if the carriers are

mainly holes, then the FET is a p-type transistor. In theory, the type of metal-CNT contact depends on the difference in work function between the metal electrode and the CNTs. However, due to the physical and chemical properties of the electrodes in contact with CNTs [19], p-type CNTFETs are more common.

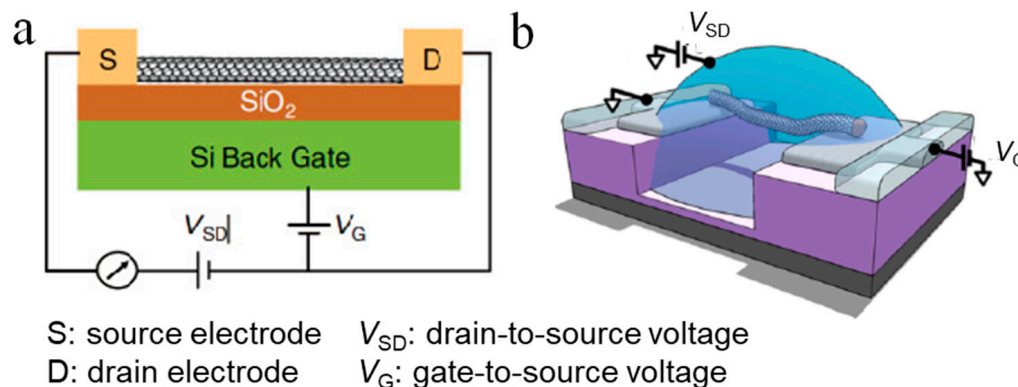


Figure 2. Illustration of CNT-based field-effect transistors (FETs) for sensing. (a) Schematic representation of a general CNTFET [17]. (b) Schematic diagram of an electrolyte-gated CNTFET [20].

CNTs have the characteristics of nanometer size, huge specific surface area, and surface effects. When a specific molecule is adsorbed on the surface of a CNTs, it causes the energy band of the CNTs to bend and affect its electronic structure, which would further cause the change of transport characteristics of CNTs. The change provides the possibility of CNTs to work as sensitive materials.

The FET-based chemical sensor and biosensor use the basic characteristics of the transistor to convert difficult-to-detect high-resistance changes into easily-detectable changes in current. The sensitivity of the sensor can be adjusted by appropriately selecting the gate operating voltage of the device. The single-walled CNTs (SWCNTs) can be divided into metal type and semiconductor type, and the FET-based chemical sensor and biosensor are prepared by using the resistance response characteristic of semiconductor SWCNTs to the adsorbed chemical.

When the chemical molecules or biological material are adsorbed on the surface of semiconductor-type CNTs, electron transfer occurs, which changes their electrical conductivity, which provides a theoretical basis for CNTs as good sensor materials. The multi-walled CNTs (MWCNTs) have a multi-layered tubular structure, so the MWCNTs have a more complex chemical adsorption mechanism than the SWCNTs. In addition, the MWCNTs lack carbon band gaps or have narrow band gaps; the tube is mainly metallic so that the adsorption of the chemical molecules has little effect on the electrical conductivity. Therefore, the conductivity of the MWCNTs is not as sensitive as that of SWCNTs, but it has been shown that the MWCNTs still have excellent sensing characteristics to substances such as water vapor [21], NH_3 [22,23], NO_2 [18], and O_2 [24,25].

The SWCNTs have shown great advantages in FET-based nanosensors. Paolo et al. [26] reported the application of CNTFETs in gas sensors. Whether for a single CNT FET or a CNT-thin film FET, the main sensing mechanism is derived from gas adsorption on the carbon tubes/metals—the modulation of the Schottky barrier at the electrodes.

3.2. Electrolyte-Gated CNTFETs

The biosensors based on electrolyte-gated FETs, also known as liquid gate FETs, have attracted increasing attention due to their advantages of easy processing [27], low cost [28], good flexibility [29], good biocompatibility, and low operating voltage. Figure 2b shows a typical configuration of an electrolyte-gated CNTFET [20], in which the electrolyte is used instead of the dielectric layer material to directly contact the gate electrode and the channel. The biggest difference between the working principle of the electrolyte-gated FET and the conventional FET is that the gate electrode regulates the channel current through

the electrolyte solution. The biggest advantage of electrolyte-gated FETs is the huge two-electron layer effect of the electrolyte [30,31], which enables the sensor to obtain the same current with a smaller gate voltage and usually can work at a rather low voltage (1V). This can avoid undesired electrochemical reactions, such as decomposition of water, damage to biological activity, etc.; thus, it can be used to detect important biological samples in a solution environment [32,33].

According to whether the ions in the electrolyte can penetrate the semiconductor channel layer, the electrolyte-gated FET can be divided into an electrostatically coupled FET and an electrochemically doped FET. Taken the p-type electrolyte-gated FET as an example, we explain these two different working mechanisms as follows. (1) Electrostatically coupled FETs. Under negative gate bias, cations in the electrolyte migrate to the gate/electrolyte interface, while the anions move to the electrolyte/channel interface, and an electric double layer is formed at the respective interface. The capacitance of the entire sensor can be equivalent to two electric double-layer capacitors connected in series. Usually, the capacitance at the electrolyte/channel interface is small, so this capacitance determines the total capacitance. Under negative bias, anions accumulated at the electrolyte/channel interface in the electrolyte induce holes of equal charge amount in the p-type channel. Under the action of the source-drain voltage, holes move in the channel to form a source-drain current. In this process, the anions in the electrolyte are always at the electrolyte/channel interface and do not penetrate the semiconductor channel layer. The holes in the channel are completely generated by the electrostatic coupling of the electric double-layer capacitance. (2) Electrochemically doped FETs. Under negative bias, cations in the electrolyte migrate to the gate/electrolyte interface, while anions migrate to the electrolyte/channel and penetrate the interface into the semiconductor channel layer. The entering anions would cancel or compensate some of the holes. This process is called electrochemical doping and occurs mostly at the electrolyte–polymer semiconductor interface. Both these two methods are often used in CNTFETs.

According to different analytes, the application of electrolyte-gated CNTFETs in chemical and biological sensors mainly includes ion sensors, small molecule sensors, protein sensors, DNA sensors, bacterial sensors, cell sensors, etc. Because the electrolyte-gated FET sensor works in a solution environment, it is particularly important to investigate the interaction between ions and CNTs. According to the interaction between ions and CNTs, ion redox, chloride ion detection, nucleic acid aptamers, and ion-selective membranes can be used for electrolyte-gated CNTFET for ion detection. For example, electrolyte-gated FET with single-walled CNTs could be used to detect redox ions [34]. It was found that ions with redox ability affect the conductivity of CNT channels mainly by adjusting the electrochemical potential of the solution. Boussaad et al. [35] prepared electrolyte-gated CNTFET sensors and studied their response to $K_3Fe(CN)_6/K_4Fe(CN)_6$, K_2IrCl_6/K_3IrCl_6 . It was found that redox ions can not only regulate the electrochemical potential of the solution, but also directly conduct a redox reaction with the CNT, thereby regulating the conductivity of the CNT channel.

4. CNTFET-Based Chemical Sensors

4.1. Gas Sensors

The CNTFET-based sensor can provide a high specific surface area for gas adsorption because almost all atoms are exposed to the gas environment, which is helpful in improving the response sensitivity. No matter as a single CNT FET or a CNT thin film FET, the main sensing mechanism is derived from gas adsorption on CNTs/metals. Unlike polycrystal line materials such as metal oxides, CNTs can avoid sensor poisoning and improve the long-term stability of the device. CNTFET-based gas sensors can detect gas molecules such as water vapor, NO_2 , NH_3 , H_2 , H_2S , C_2H_5OH and methanol vapor, with very good detection limits and detection ranges, and their anti-noise capabilities and detection accuracy are significantly better than traditional gas sensors, and even can detect a single gas molecule [36]. Some recent works are summarized in Table 1.

The research on carbon nanotube gas sensors began with the work published by Kong [37]. Gas-sensitivity characteristics of CNTFET to NH_3 and NO_2 were investigated by Tans [38]. The research found that, when exposed to NH_3 , the Fermi level in the p-type CNTFET shifts to the conduction band, which results in a decreased hole concentration and thus a decreased conductance; when exposed to NO_2 , the Fermi level shifts to the valence band, and the hole concentration and the conductance increases. In addition, the transfer curve would show a relative difference when exposed to different concentrations of the same gas.

Table 1. The research on CNTFET for gas detection.

Analytes	Detection Limit	Response Time	Author	References
NO_2	200 ppm	2–10 s	Kong	[37]
NO_2	ppb level	Not reported	Sacco	[18]
NO_2	10 ppb	Not reported	L. Valentini	[39]
NO_2	125 ppt	Not reported	Kumar	[40]
NH_3	1%	1–2 min	Kong	[37]
Carbonyl Chloride	630 nm/refractive index unit	Not reported	Ghodrati	[41]
Methanol	1.3%	Not reported	Badhulika	[42]
Ethanol	5.95%	Not reported	Badhulika	[42]
Ethanol	50 ppm	Nor reported	Sean Brahim	[43]
Ethanol	1.67%	Not reported	S. J. Young	[44]
Methyl ethyl ketone	3%	Not reported	Badhulika	[42]
Nitrogen dioxide	1 ppm	Not reported	Radouane	[45]
Carbon monoxide	20 ppm	Not reported	Radouane	[45]
Ammonia	1%	0.1 s	panelF.Villalpando-Páez	[46]
Ammonia	100 ppb	15 min	Qifei Chang	[47]

Figure 3 shows several representative works of gas sensing with a CNTFET. Slobodan [48] reported the detection of methanol gas by using MWCNTs. The reaction of MWCNT FETs to methanol after treatment in acidic KMnO_4 increased by about 12–46%, as shown in Figure 3a. Sattari [48] spin-coated a composite of MWCNTs and polyaniline (PANI) on glass and silicon substrates and performed sensor measurements on methane gas. The MWCNT–PANI membrane presents greatly enhanced sensitivity to methane gas compared to the pure PANI membrane, [49] as shown in Figure 3b. Badhulika [42] used SWCNTs with poly(3,4-ethylenedioxythiophene) polystyrene sulfonate (PEDOT:PSS) coating to make volatile organic compounds (VOCs) gas sensors. For saturated vapors of methanol (Figure 3c), ethanol and methyl ethyl ketone, the detection limits are 1.3%, 5.95% and 3%, respectively. Zhao [50] pointed out that NO_2 and NH_3 gases have strong enough interactions with CNTs (chemical adsorption), while other gases with low adsorption energy only bind to CNTs by Van der Waals force (physical adsorption). Woods [51] points out that the molecules of volatile organic compounds (VOCs) interact weakly with CNTs. The weaker interaction between VOCs and CNTs reduces the performance of their gas sensors. Therefore, in monitoring VOCs, increasing the reactivity of CNTs is a key point.

Different approaches have been studied for the modification of CNTs to improve the sensing performances, including using Au nanoparticles, certain solutions, polymers, metals, or impurities.

CNTFET [52] gas sensors pretreated with Au nanoparticles prepared by electrophoretic deposition method have high sensitivity and selectivity to NO_2 and H_2S , as shown in Figure 3d. In S. J. Young's study [44], a 10-nm thick Fe layer was sputtered followed by synthesizing CNTs, and the fabricated CNT ethanol gas sensors can reach a sensitivity of 1.67% under 800 ppm ethanol vapor concentration at room temperature, as shown in Figure 3e. Radouane [45] used MWCNTs decorated with tin oxide for sensing 1 ppm

nitrogen and 20 ppm monoxide. This hybrid sensor has an excellent sensitivity and significantly eliminates the moisture cross-sensitivity.

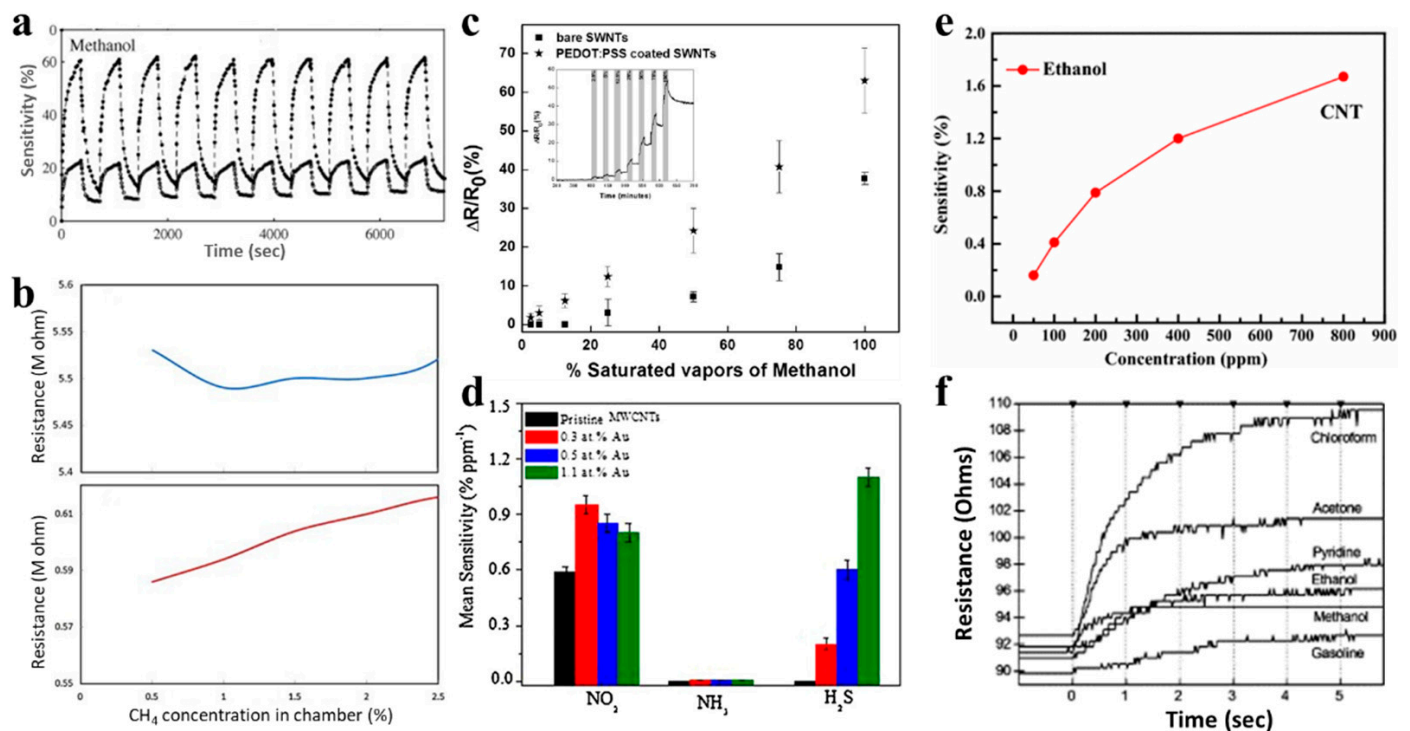


Figure 3. CNTFET-based gas sensor. (a) The response of CNTFET to methanol with (open symbols) and without (filled symbols) KMnO_4 treatment [48]. (b) The response of polyaniline (PANI) (top) and multi-walled CNT (MWCNT)-PANI (bottom) membranes to methane gas [49]. (c) The response of SWCNTs with PEDOT:PSS coating to methanol [42]. (d) Selective response of CNTFET sensor functionalized with Au nanoparticles [52]. (e) CNTFET ethanol gas sensors functionalized with 10 nm Fe layer [44]. (f) Aligned CN_x nanotubes sensors in response to different vapors [46].

Impurity atoms have been incorporated into CNTs to improve their gas sensing performance, such as pyridine-like sites, boron, and nitrogen atoms. F.Villalpando-Páez [46] reported aligned CN_x nanotubes sensors that are capable of sensing the toxic species because of the presence of highly reactive pyridine-like sites on the tube surface which can strongly bind to ammonia, acetone and OH groups (Figure 3f) and further change their density of states. This type of sensor is both responsive and reusable at the same time. To overcome the reliability problem owing to the weak van der Waals interaction between the SWCNTs and the doped materials, Shu Peng [53] reports a concept of a brand new type of CNT-based gas sensor by doping the impurity atoms (such as boron, nitrogen atoms) into SWCNTs.

4.2. H_2O_2 Detection

H_2O_2 is a by-product of most enzyme-catalyzed reactions and is closely related to the occurrence of many metabolites in the body, such as glucose, lactate, cholesterol. Thus, the detection of H_2O_2 can be correlated to the concentration of these metabolites through specific enzymatic reactions. Figure 4a shows the schematic of a CNTFET sensor for H_2O_2 with the bioreceptor of concavalin A, in which H_2O_2 is intermediate of glucose reaction, and the concentration of H_2O_2 and thus the concentration of glucose can be detected by CNTFET sensor. [54] The calibrated curve in Figure 4b shows a good linear relationship between the relative resistance change of the sensor and the glucose concentration, which is tested in human plasma, revealing the potential application of the sensor for blood glucose measurements. Saumya [55] used CNTFET sensors to detect lactate (Figure 4c) and glucose (Figure 4d) via the enzymatic reaction catalyzed by glucose oxidase and lactate

oxidase, respectively, with H_2O_2 as a product of the reaction. This method possesses a good monitoring sensitivity, and a decent detection limit of pico molar (μM) levels.

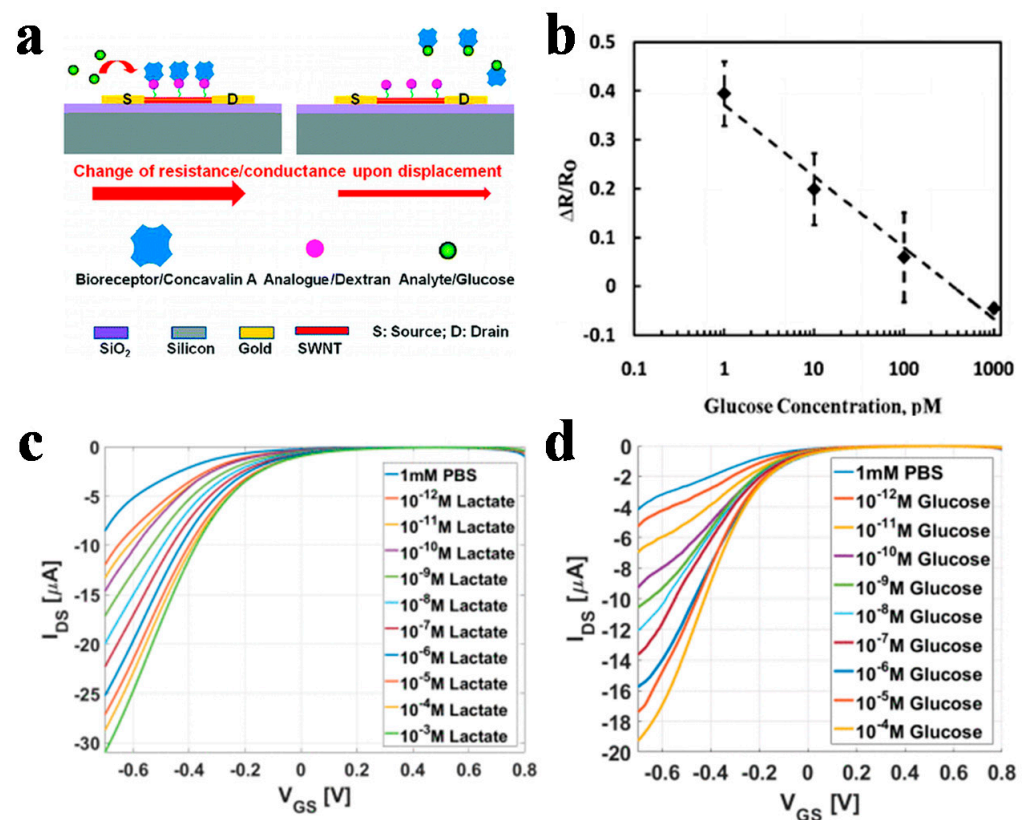


Figure 4. CNTFET-based H_2O_2 sensor. (a) Schematic of a CNTFET for glucose sensing via the detection of H_2O_2 and (b) its relative resistance change in response to different glucose concentrations [54]. The change of current of CNTFETs in response to (c) different lactate and (d) glucose concentrations via enzymatic reactions with H_2O_2 as a by-product [55].

5. CNTFET-Based Biological Sensors

Label-free biosensors are very attractive due to their simple procedure, high sensitivity, rapid detection, easy of miniaturization and integration. The CNT with a 1-D nanostructure has shown a strong sensitivity to the surface adsorption of many chemicals and biomolecules. This enables the CNT to be an ideal material for constructing label-free biosensors to detect proteins [56,57], nucleic acids, cells, and viruses [58–60].

5.1. Protein Detection

CNTs can be functionalized with specific antibodies to detect different proteins. When proteins are bound onto CNTs by receptors on the surface, it leads to a change of source and drain current and voltage. Some recent works are summarized in Table 2. Boussaad [61] detected the non-covalent adsorption amount of cytochrome c in situ by monitoring the conductance change in semiconductor CNTs. The basic structure of a SWCNT device is shown in Figure 5a. The detection sensitivity is high, up to 20 protein molecules/carbon tubes, as shown in Figure 5b. The possible reason for the change is that the positively-charged cytochrome c reduces the electronic load of the p-type semiconductor CNTs, resulting in a decrease in conductance. Figure 5c shows the illustration of the CNTFET sensor for prostate-specific antigen (PSA) detection [62]. PSA monoclonal antibody was immobilized on the SWCNT surface and PSA can be bound to the antibody for recognition. When the device was exposed to 1.4-nM PSA, the current was changed about 2% as shown in Figure 5d. Wang [63] used an antibody-functionalized CNTFET biosensor to detect in situ chromogranins (CgA) released from neurons, as shown in Figure 5e,f, where small current

increase was observed when neurons were attached onto the CgA antibody-modified SWCNT FET. Marcin [64] fabricated sorted CNT networks with a nanobody receptor for protein detection up to 1 pM.

Table 2. The research on CNTFET for protein detection.

Analytes	Detection Limit	Sensitivity	Author	References
Dopamine	0.062 μ M	Not reported	Haiyan Cheng	[65]
Dopamine	15 nM	Not reported	Jinyan Cheng	[66]
Dopamine	0.87 nM	Not reported	Qitong Huang	[67]
Specific protein detection	0.1 pM	Not reported	Marcin	[64]
Non-structural protein 1 of the dengue virus	2 ng/mL	Not reported	sAna Carolina M.S.Dias	[68]
Prostate specific antigen	1 pg/mL	Not reported	Naimish P. Sardesai	[69]
IL-6	0.25 pg/ mL	Not reported	Naimish P. Sardesai	[69]
Hexahistidine-tagged capture proteins	10 pM	600 s	Jin-Ho Ahn	[70]
Pig serum albumin	2.06 μ mol/L	Not reported	Atsuhiko Kojima	[71]
Urokinase plasminogen activator	25 nM	Not reported	Ryan M. Williams	[72]

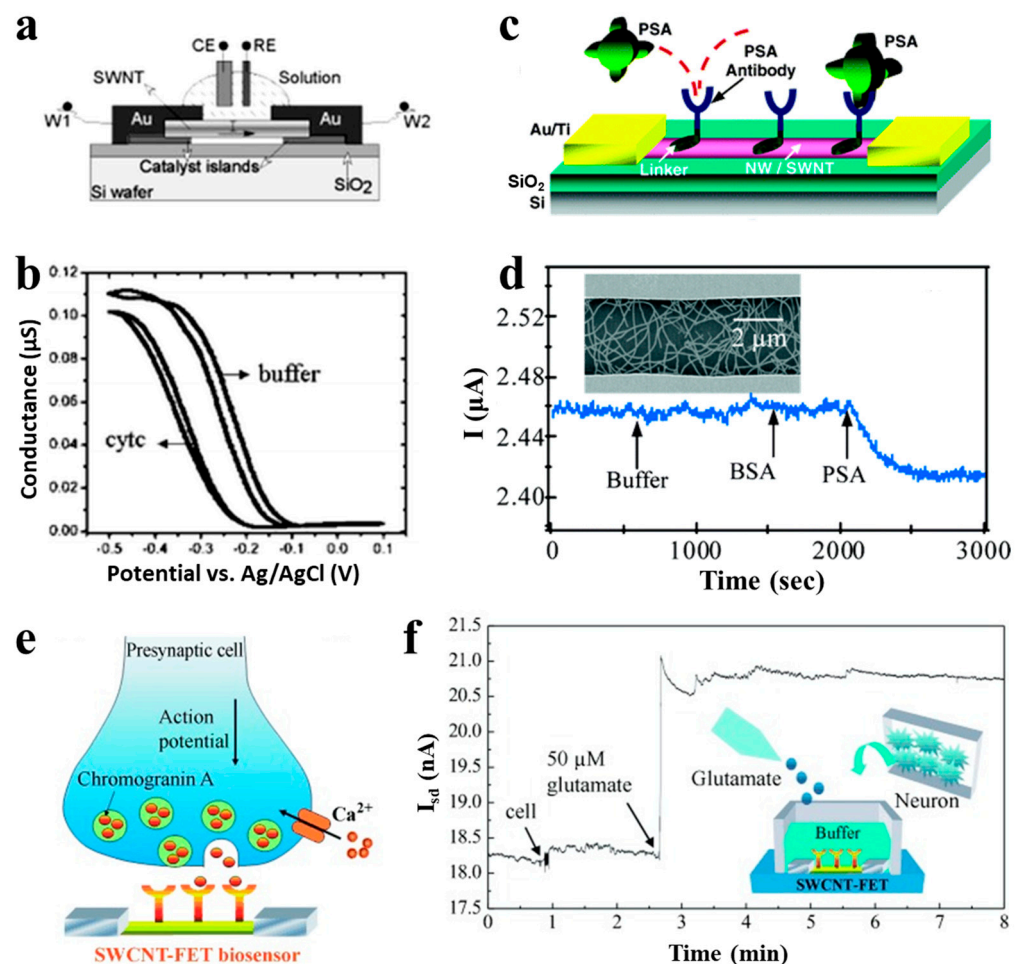


Figure 5. CNTFET-based sensors for protein detection. (a) Schematic illustration of a SWCNT device for cytochrome c detection [61]. (b) Conductance of the CNTFET as a function of the electrochemical potential in phosphate buffer and 200 μ M cytochrome c in buffer. (c) Schematic device diagram and (d) current change of CNT nanosensors for prostate-specific antigen (PSA) detection [62]. (e) Schematic illustration of chromogranin (CgA) released from neurons and (f) its detection by monitoring the current change of a CgA antibody-modified CNTFET [63].

5.2. Cell Detection

The CNTs can be functionalized with the specific antibodies to detect different cells, such as bacterial, pathogenic yeast, or mammalian cells. The living cell could also be absorbed on the CNT surface because of physical or chemical reasons, which could lead to the change of transfer curve, make it possible for detection.

Villamizar [73] reported a study using Salmonella antibodies to functionalize CNT-FETs for Salmonella detection at a minimum concentration of 100 colony-forming units (cfu)/mL, as shown in Figure 6a. In addition, a similar method has been used to construct biosensors by functionalizing CNTFETs with Escherichia coli aptamer for Escherichia coli detection [74]. The conductivity of the device is reduced by more than 50% after the Escherichia coli is captured (Figure 6b).

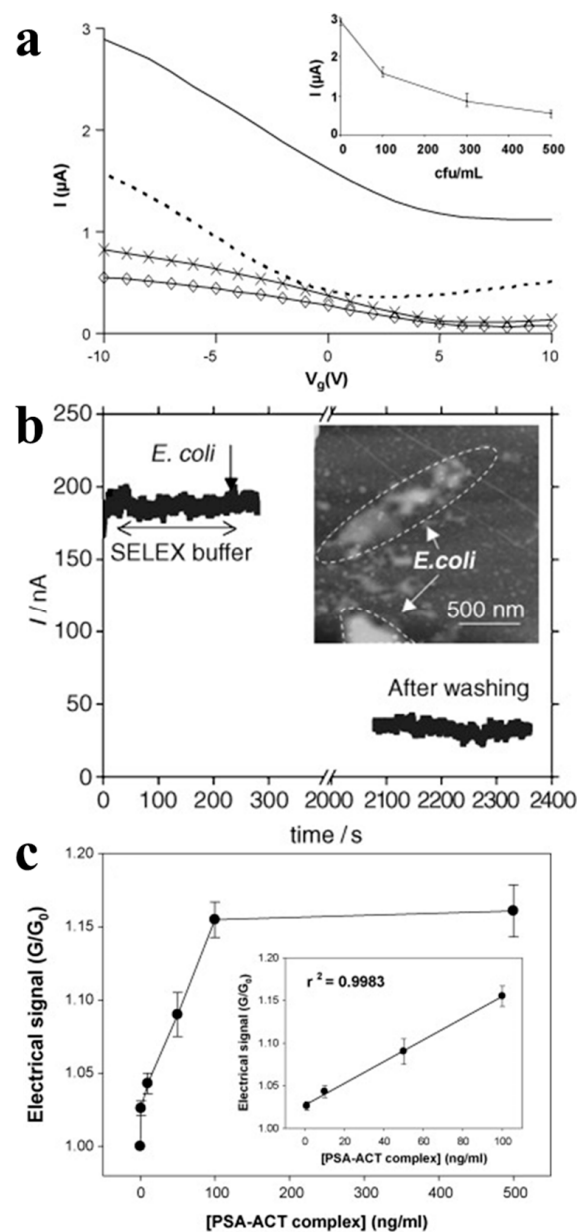


Figure 6. CNTFET-based sensors for cell detection. (a) From top to bottom, transfer curves before and after exposure to Salmonella with concentrations of 100 cfu/mL, 300 cfu/mL and 500 cfu/mL, respectively [73]. (b) Current change of the CNTFET for Escherichia coli detection [74]. (c) Prostate-specific antigen PSA-ACT complex detection on the CNTFETs modified with a 1:3 linker to spacer ratio [75].

Kim [75] proposed a label-free protein biosensor based on a functionalized CNTFET for detecting the prostate cancer marker, PSA- α_1 -antichymotrypsin (PSA-ACT complex), as shown in Figure 6c. They functionalized the CNTFET with a 1:3 ratio of linker-to-spacer. Owing to addition of spacers on the CNT surface, this approach could widen the distance between the receptors. Thus, the negatively charged proteins can approach the channel within the distance of the Debye length to further affect the conductance of the CNTFET more easily. This results in a sensitive detection of 1.0 ng/mL.

5.3. Nucleic Acid Detection

Nucleic acid analytes, such as DNA and RNA, can be effectively combined with CNTFET biosensors. The detection of DNA by sequence-specific hybridization is a common detection strategy to ensure the specificity of biosensors. The FET biosensor can functionalize complementary DNA/RNA/peptide nucleic acid (PNA) strands to the sensor surface, so that the complementary binding target strand can produce the specific binding to ensure its selectivity and produce a detectable electrical response. Some recent work has been summarized in Table 3.

Table 3. The research on CNTFET for Nucleic acid-based analyte detection.

Analytes	Receptors	Detection Limit	Author	References
12-mer ssRNA	12-mer PNA	Not Reported	Martínez	[76]
10-mer ssDNA	10-mer ssDNA probe	Single molecule	Sorgenfrei	[77]
microRNA-122a	p19 protein	1 aM	Ramnani	[78]
DNA	Amino-functionalized probe DNA	Attomolar level	Tetiana Kurkina	[79]
ssDNA	ssDNA probe	2 nM	Stine	[80]
ssDNA	Peptide nucleic acid probe	100 fM	Cai	[81]
ssDNA	ssDNA probe	<1 attomole.	ShunWang	[82]
ssDNA	ssDNA probe	<1 attomole.	ShunWang	[82]
ssDNA	ssDNA probe	2.4 nM	Yin	[83]
ssDNA	ssDNA probe	0.5 nM	Phuong DinhTam	[84]
ssDNA	ssDNA probe	0.7 fM	B Zribi	[85]
ssDNA	Amine-modified DNA detection probe	0.1 nM	Wanwei Qiu	[86]
ssDNA	ssDNA	1 pM	Alexander Star	[87]
ssDNA	ssDNA	100 fM	Xiaochen Dong	[88]
ssDNA	Amino modified PNA	6.8 fM	Kenzo Maehashi	[89]
ssDNA	Peptide nucleic acid probe	10 fM	Zheng	[90]

As shown in Figure 7a, the sensing of DNA relies on the binding of DNA double-strand which has an effect on the CNTFET transfer curve [91]. The concentration of DNA will be detected by the shift degree of the transfer curves. Star [87] reported a CNT network FET for the detection of a specific DNA sequence.

A sequence. This kind of sensor showed the ability to recognize the target DNA sequences by immobilizing the synthetic oligonucleotides. It was further approved that ssDNA was successfully immobilized and hybridized with the target subsequent DNA by utilizing fluorescence-labeled oligonucleotides. The sensor had a detection limit of 1 nM (Figure 7b), and was both highly sensitive and low-cost. Dong [88] further improved the CNTFET DNA sensor by labeling a reporter DNA probe with Au nanoparticles in the hybridization step, and the detection process is illustrated in Figure 7c. MAHASHI [89] demonstrated a CNTFET-based DNA sensor which covalently immobilized amino modified PNA oligonucleotides at 5' onto the Au surface of the back gate. The sensor can detect DNA as low as 6.89 fM.

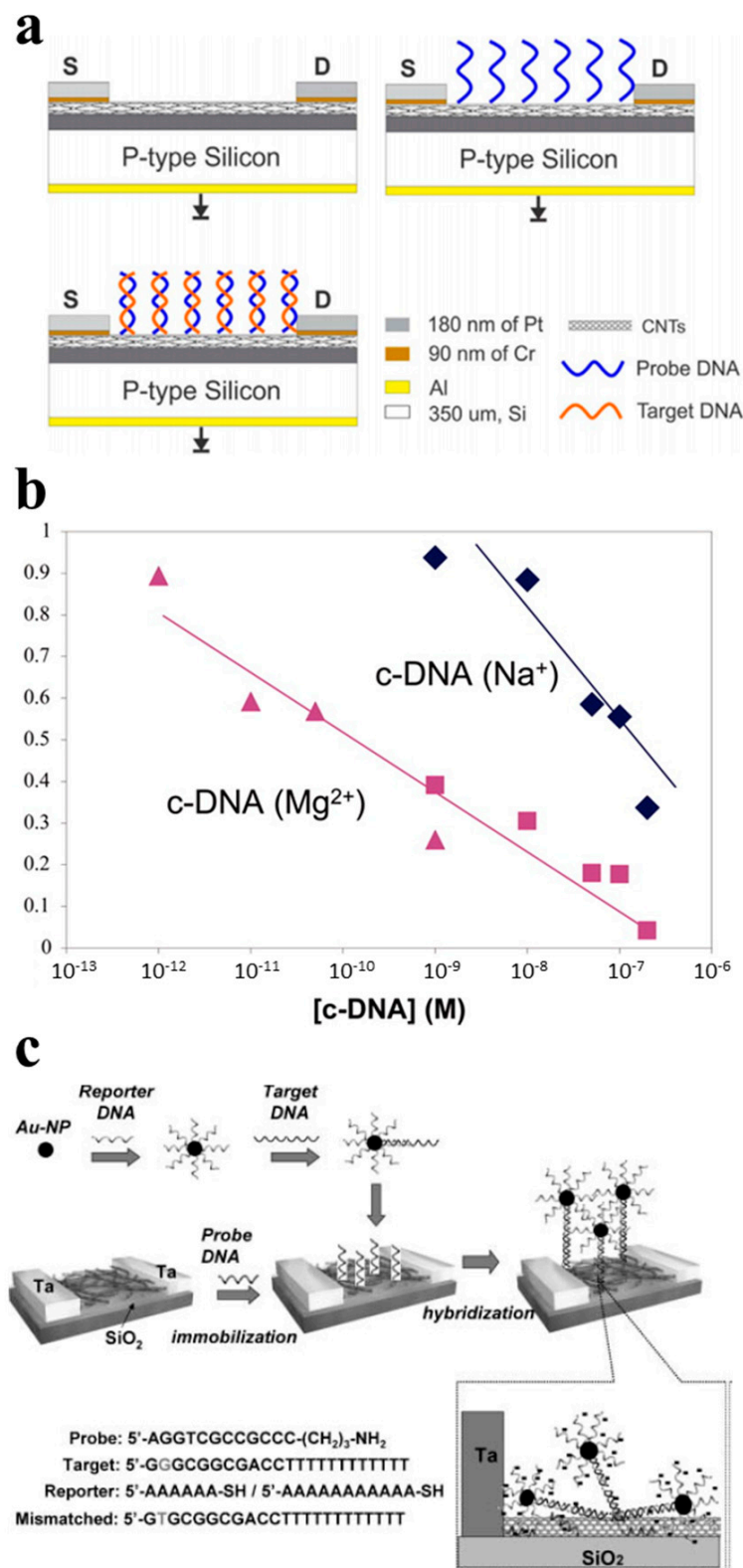


Figure 7. CNTFET-based sensors for DNA detection. (a) Working principle of CNTFET-based DNA sensors [91]. (b) Normalized conductance as a function of target DNA concentrations [87]. (c) Schematic illustration of DNA detection with reporter DNA conjugated with Au nanoparticles [88].

5.4. Virus Detection

CNTFET-based biosensors can be used for the monitoring of a variety of viruses. The virus sensing is usually based on detecting the DNA of the virus through the immobilization

of DNA or PNA, or directly detecting the virus through the immobilization of the antibody or peptide. Some recent works are summarized in Table 4. Dastagir [92] constructed an FET sensor using functional CNT as the channel material to monitor the sequence of the hepatitis c virus (HCV) (Figure 8a). They used PNA, which possesses high affinity and stability for RNA hybridization, to perform CNT functionalization, and a sensor that could carry on an unlabeled detection with a detection limit of 0.5 pM, as shown in Figure 8b.

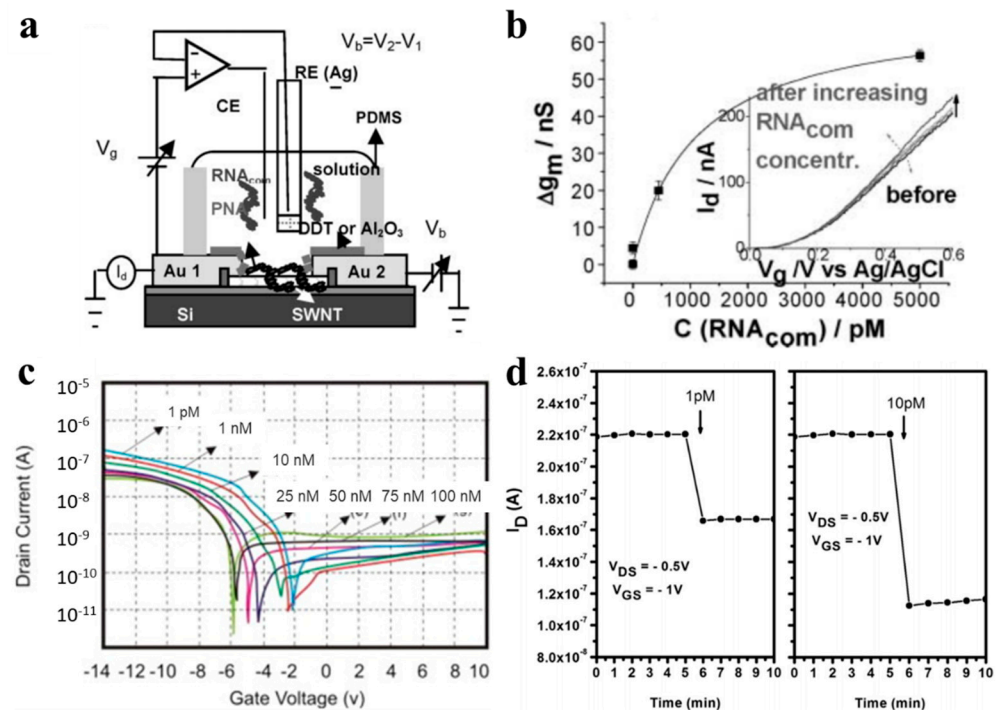


Figure 8. CNTFET-based sensors for virus detection. (a) The experimental setup and (b) transconductance change vs. RNA concentrations of the hepatitis c virus (HCV) sensor [92]. (c) Detection of H5N1 at different concentrations [93]. (d) Response to influenza type A virus DNA within 1 min [91].

Thu [93] reports on a CNTFET for the selective detection of H5N1. In this sensor, the CNT network acts as a conductor channel, producing signal changes when the virus binds to specific receptors on the CNT surface. The specific DNA sequence was a receptor bound to the H5N1 virus, with a detection limit of up to 1.25 pM and a sensitivity of 0.28 nM/nA, as shown in Figure 8c. Tran [91] reported a CNTFET-based sensor for the detection of influenza type A virus DNA. They used an immobilized single DNA strand on the CNT network as the probe which would hybridize with the analyte DNA to further alter the ion concentration on the surface. As the ion concentration changes, the transfer curve of the CNTFET changes. This sensor has a detection limit of 1 pM within a linear detection range from 1 pM to 10 nM and also shows superior responsiveness in less than one minute, the response time is shown in Figure 8d. Fatin [94] demonstrates a MWCNT-based sensor for HIV-1 virus which utilized a split RNA aptamer as the detection probe. The sensor has a detection limit of 600 pM.

Table 4. The research on CNTFET for virus detection.

Analytes	Detection Limit	Sensitivity	Author	References
H5N1 virus	1.25 pM	0.28 nM/nA	Vu	[93]
Influenza A virus	10 µM	Not reported	Thi	[87]
Avian influenza virus	1 EID ₅₀ (50% embryo infectious doses)/mL	Not reported	Yin-Ting Yeh	[95]
H1N1	180 TCID ₅₀ (50% tissue culture infective dose)/mL	Not reported	Dongjin Lee	[96]
Hepatitis C virus	pM level	Not reported	Tawab Dastagir	[92]
Dengue virus	2 ng mL ⁻¹	Not reported	Naimish P. Sardesai	[68]
M13-bacteriophage	0.5 pM	Not reported	HS Mandal	[97]
Dengue virus	0.1 µg mL ⁻¹	Not reported	Mízia M. S. Silva	[98]
Hepatitis B	0.03 ng mL ⁻¹	Not reported	Diego G.A.Cabral	[99]
Hepatitis B	<1 attomole	Not reported	ShunWang	[6]
SARS-CoV-2	35 mg/L	Not reported	Rebecca L. Pinals	[100]
Hepatitis C	0.7 fM	Not reported	B Zribi	[85]
Papilloma virus	<1 attomole	Not reported	ShunWang	[82]
Human papilloma virus	130 µA/V	Not reported	Gopinath	[101]

6. Conclusions

The CNTs have shown the extraordinary electrical and sensing properties, and we here review the recent progress of the CNTFET-based chemical and biological sensors. The CNTs generally go through covalent or non-covalent surface functionalization, in order to generate sufficient or selective sensing signals. The configurations include the general FET structure and electrolyte-gated FETs. The CNTFET-based sensors have been applied for the effective chemical sensing of various gases or H₂O₂. The bioreceptor functionalization of the CNTFET enables the construction of various biological sensors for detecting a variety of proteins, cells, nucleic acids, and viruses. Due to the nanoscale channel with a large surface to volume ratio and an atomically thin body to provide ideal electrostatic control, a small change of the surrounding environment can significantly modify CNTFETs' electrical characteristics, and, thus, a small concentration of the target analyte that can bind to the surface of the channel can result in a detectable change of the electrical signal. So, these sensors generally exhibit a highly sensitive detection of the target analyte. We expect the CNT transistor-based sensors to deepen the fundamental understanding of the interaction of the analyte with the CNTFET, as well as explore a wide range of applications in healthcare, environmental, and food. Although the progress for the CNTFET-based chemical and biological sensors is promising, the field still faces the critical challenges for practical applications, and these include (1) the unstable electrical performance of the CNTFET over time; (2) the fluctuation of the sensing performance by small variation of the surroundings, such as the buffer condition; and (3) the non-linear calibration curve between the electrical signal and the concentration of the analyte. These issues hamper the realization of portable and miniaturized systems using FET transduction and significant lowering of the manufacturing cost will also be critical to allow CNTFET-based sensors to be marketed.

Author Contributions: Conceptualization, Y.C. and Y.H.; methodology, X.Y., Y.Z., W.J., Y.H. and Y.C.; writing—original draft preparation, X.Y., Y.Z., W.J., Y.H. and Y.C.; writing—review and editing, X.Y., Y.Z., W.J., Y.H. and Y.C.; supervision, Y.C. and Y.H. All authors have read and agreed to the published version of the manuscript.

Funding: This research was funded by the National Natural Science Foundation of China (grant numbers 52072007 to Y.C. and 61971012 to Y.H.), the Clinical Medicine Plus X- Young Scholars Project, Peking University, the Fundamental Research Funds for the Central Universities.

Institutional Review Board Statement: Not Applicable.

Informed Consent Statement: Not Applicable.

Data Availability Statement: Not Applicable.

Conflicts of Interest: The authors declare no conflict of interest.

References

1. Khamfoo, K.; Inyawilert, K.; Wisitsoraat, A.; Tuantranont, A.; Phanichphant, S.; Liewhiran, C. Formaldehyde sensor based on FSP-made AgOx-doped SnO₂ nanoparticulate sensing films. *Sensor. Actuat. B Chem.* **2020**, *309*, 127705. [[CrossRef](#)]
2. Nam, B.; Ko, T.-K.; Hyun, S.-K.; Lee, C. CO Sensing Properties of Chemiresistive In₂O₃/SnO₂ Composite Nanoparticle Sensors. *J. Nanosci. Nanotechnol.* **2020**, *20*, 4344–4348. [[CrossRef](#)] [[PubMed](#)]
3. Sebok, D.; Dekany, I. ZnO₂ nanohybrid thin film sensor for the detection of ethanol vapour at room temperature using reflectometric interference spectroscopy. *Sensor. Actuat. B Chem.* **2015**, *206*, 435–442. [[CrossRef](#)]
4. Baccarin, M.; Ciciliati, M.A.; Oliveira, O.N., Jr.; Cavalheiro, E.T.; Raymundo-Pereira, P.A. Pen sensor made with silver nanoparticles decorating graphite-polyurethane electrodes to detect bisphenol-A in tap and river water samples. *Mater. Sci. Eng. C* **2020**, *114*, 110989. [[CrossRef](#)]
5. Raymundo-Pereira, P.A.; Baccarin, M.; Oliveira, O.N., Jr.; Janegitz, B.C. Thin films and composites based on graphene for electrochemical detection of biologically-relevant molecules. *Electroanalysis* **2018**, *30*, 1888–1896. [[CrossRef](#)]
6. Cui, J.; Zhang, J.; He, X.; Mei, X.; Wang, W.; Yang, X.; Xie, H.; Yang, L.; Wang, Y. Investigating interfacial contact configuration and behavior of single-walled carbon nanotube-based nanodevice with atomistic simulations. *J. Nanopart. Res.* **2017**, *19*, 110. [[CrossRef](#)]
7. Yang, W.D.; Li, Y.D.; Wang, X. Scale-dependent dynamic-pull-in of functionally graded carbon nanotubes reinforced nanodevice with piezoelectric layer. *J. Aerospace Eng.* **2017**, *30*, 04016096. [[CrossRef](#)]
8. Ni, D.; Zhang, J.; Wang, X.; Qin, D.; Li, N.; Lu, W.; Chen, W. Hydroxyl radical-dominated catalytic oxidation in neutral condition by axially coordinated iron phthalocyanine on mercapto-functionalized carbon nanotubes. *Indus. Eng. Chem. R.* **2017**, *56*, 2899–2907. [[CrossRef](#)]
9. Rezaei, S.J.T.; Khorramabadi, H.; Hesami, A.; Ramazani, A.; Amani, R.; Ahmadi, R. Chemoselective reduction of nitro and nitrile compounds with magnetic carbon nanotubes-supported Pt(II) catalyst under mild conditions. *Ind. Eng. Chem. Res.* **2017**, *56*, 12256–12266. [[CrossRef](#)]
10. Liu, H.; Chen, J.-G.; Wang, C.; Liu, Z.-T.; Li, Y.; Liu, Z.-W.; Xiao, J.; Lu, J. Immobilization of cyclometalated iridium complex onto multiwalled carbon nanotubes for dehydrogenation of indolines in aqueous solution. *Ind. Eng. Chem. Res.* **2017**, *56*, 11413–11421. [[CrossRef](#)]
11. Dalton, A.B.; Stephan, C.; Coleman, J.N.; McCarthy, B.; Ajayan, P.M.; Lefrant, S.; Bernier, P.; Blau, W.J.; Byrne, H.J. Selective interaction of a semiconjugated organic polymer with single-wall nanotubes. *J. Phys. Chem. B* **2000**, *104*, 10012–10016. [[CrossRef](#)]
12. Stobinski, L.; Tomasik, P.; Lii, C.Y.; Chan, H.H.; Lin, H.M.; Liu, H.L.; Kao, C.T.; Lu, K.S. Single-walled carbon nanotube—Amylopectin complexes. *Carbohydr. Polym.* **2003**, *51*, 311–316. [[CrossRef](#)]
13. Islam, M.F.; Rojas, E.; Bergey, D.M.; Johnson, A.T.; Yodh, A.G. High weight fraction surfactant solubilization of single-wall carbon nanotubes in water. *Nano Lett.* **2003**, *3*, 269–273. [[CrossRef](#)]
14. Cui, D.; Ozkan, C.S.; Ravindran, S.; Kong, Y.; Gao, H. Encapsulation of pt-labelled DNA molecules inside carbon nanotubes. *Mech. Chem. Biosyst. MCB* **2004**, *1*, 113–121. [[PubMed](#)]
15. Kim, H.; Seo, J.; Seong, N.; Lee, S.; Lee, S.; Kim, T.; Hong, Y. Multidipping technique for fabrication time reduction and performance improvement of solution-processed single-walled carbon nanotube thin-film transistors. *Adv. Eng. Mater.* **2020**, *22*, 1901413. [[CrossRef](#)]
16. Chen, J.; Zhang, B.; Dang, X.; Zheng, D.; Ai, Y.; Chen, H. A nanocomposite consisting of etched multiwalled carbon nanotubes, amino-modified metal-organic framework UiO-66 and polyaniline for preconcentration of polycyclic aromatic hydrocarbons prior to their determination by HPLC. *Mikrochim. Acta* **2020**, *187*, 78. [[CrossRef](#)]
17. Moghaddam, S.; Ghoreishi, S.S.; Yousefi, R.; Aderang, H. Quantum simulation of a junctionless carbon nanotube field-effect transistor under torsional strain. *Superlattice. Microst.* **2020**, *138*, 106239. [[CrossRef](#)]
18. Sacco, L.; Forel, S.; Florea, I.; Cojocar, C.-S. Ultra-sensitive NO₂ gas sensors based on single-wall carbon nanotube field effect transistors: Monitoring from ppm to ppb level. *Carbon* **2020**, *157*, 631–639. [[CrossRef](#)]
19. Choi, Y.; Kim, J.-H.; Qian, C.; Kang, J.; Hersam, M.C.; Park, J.-H.; Cho, J.H. Gate-tunable synaptic dynamics of ferroelectric-coupled carbon-nanotube transistors. *ACS Appl. Mater. Inter.* **2020**, *12*, 4707–4714. [[CrossRef](#)]
20. Sharf, T.; Wang, N.-P.; Kevek, J.W.; Brown, M.A.; Wilson, H.; Heinze, S.; Minot, E.D. Single electron charge sensitivity of liquid-gated carbon nanotube transistors. *Nano Lett.* **2014**, *14*, 4925–4930. [[CrossRef](#)]
21. Lapointe, F.; Ding, J.; Lefebvre, J. Carbon Nanotube Transistors as Gas Sensors: Response differentiation using polymer gate dielectrics. *ACS Appl. Poly. Mater.* **2019**, *1*, 3269–3278. [[CrossRef](#)]
22. Eberle, S.; Roman, C.; Hierold, C. Effect of varying gate distance on the threshold voltage shift in carbon nanotube field effect transistor gas sensors. *Microelectron. Eng.* **2018**, *193*, 86–90. [[CrossRef](#)]
23. Jeon, M.; Choi, B.; Yoon, J.; Kim, D.M.; Kim, D.H.; Park, I.; Choi, S.-J. Enhanced sensing of gas molecules by a 99.9% semiconducting carbon nanotube-based field-effect transistor sensor. *Appl. Phys. Lett.* **2017**, *111*, 022102. [[CrossRef](#)]
24. Sivasathya, S.; Thiruvadigal, D.J. Ab Initio study of carbon nanotube transistor-based gas sensor for NO₂ detection. *Asian J. Chem.* **2013**, *25*, S411–S413.

25. Wei, L.; Chen, H.; Wang, J.; Yuang, W.; Zhao, J.; Xu, D.; Zhang, Y. Gas Sensors based on single-walled carbon nanotube field-effect transistor. *Sensor. Mater.* **2014**, *26*, 9–17.
26. Bondavalli, P.; Legagneux, P.; Pribat, D. Carbon nanotubes based transistors as gas sensors: State of the art and critical review. *Sensor. Actuat. B Chem.* **2009**, *140*, 304–318. [[CrossRef](#)]
27. Delgado, K.P.; Raymundo-Pereira, P.A.; Campos, A.M.; Oloveira, O.N., Jr.; Janegitz, R.C. Ultralow cost electrochemical sensor made of potato starch and carbon black nanoballs to detect tetracycline in waters and milk. *Electroanalysis* **2018**, *30*, 2153–2159. [[CrossRef](#)]
28. Raymundo-Pereira, P.A.; Shimizu, F.M.; Coelho, D.; Piazzeta, M.H.; Gobbi, A.L.; Machado, S.A.; Oliveira, O.N., Jr. A nanostructured bifunctional platform for sensing of glucose biomarker in artificial saliva: Synergy in hybrid Pt/Au surfaces. *Biosens. Bioelectr.* **2016**, *86*, 369–376. [[CrossRef](#)]
29. Scuratti, F.; Bonacchini, G.E.; Bossio, C.; Salazar-Rios, J.M.; Talsma, W.; Loi, M.A.; Antognazza, M.R.; Caironi, M. Real-time monitoring of cellular cultures with electrolyte-gated carbon nanotube transistors. *ACS Appl. Mater. Interfaces* **2019**, *11*, 37966–37972. [[CrossRef](#)]
30. Dorfman, K.D.; Adrahtas, D.Z.; Thomas, M.S.; Frisbie, C.D. Microfluidic opportunities in printed electrolyte-gated transistor biosensors. *Biomicrofluidics* **2020**, *14*, 011301. [[CrossRef](#)]
31. Tin Phan, N.; Hayakawa, R.; Kilinc, V.; Petit, M.; Yemini, S.L.V.N.; Higuchi, M.; Raimundo, J.M.; Charrier, A.M.; Wakayama, Y. Electrolyte-gated-organic field effect transistors functionalized by lipid monolayers with tunable pH sensitivity for sensor applications. *Appl. Phys. Expre.* **2020**, *13*, 011005.
32. Jo, I.Y.; Park, J.-G.; Moon, J.-H.; Jung, J.Y.; Kim, D.E.; Baeg, K.-J. Low-voltage-operating complementary-like circuits using ambipolar organic-inorganic hybrid thin-film transistors with solid-state-electrolyte gate insulator. *Org. Electron.* **2019**, *75*, 105358. [[CrossRef](#)]
33. Neuper, F.; Chandresh, A.; Singaraju, S.A.; Aghassi-Hagmann, J.; Hahn, H.; Breitung, B. Tailoring threshold voltages of printed electrolyte-gated field-effect transistors by chromium doping of indium oxide channels. *ACS Omega* **2019**, *4*, 20579–20585. [[CrossRef](#)] [[PubMed](#)]
34. Larrimore, L.; Nad, S.; Zhou, X.; Abruna, H.; McEuen, P.L. Probing electrostatic potentials in solution with carbon nanotube transistors. *Nano Lett.* **2006**, *6*, 1329–1333. [[CrossRef](#)] [[PubMed](#)]
35. Boussaad, S.; Diner, B.A.; Fan, J. Influence of redox molecules on the electronic conductance of single-walled carbon nanotube field-effect transistors: Application to chemical and biological sensing. *J. Am. Chem. Soc.* **2008**, *130*, 3780–3787. [[CrossRef](#)]
36. Shirsat, M.D.; Sarkar, T.; Kakoullis, J., Jr.; Myung, N.V.; Konnanath, B.; Spanias, A.; Mulchandani, A. Porphyrin-functionalized single-walled carbon nanotube chemiresistive sensor arrays for VOCs. *J. Phys. Chem. C* **2012**, *116*, 3845–3850. [[CrossRef](#)]
37. Kong, J.; Franklin, N.R.; Zhou, C.; Chapline, M.G.; Peng, S.; Cho, K.; Dai, H. Nanotube molecular wires as chemical sensors. *Science* **2000**, *287*, 622–625. [[CrossRef](#)]
38. Tans, S.J.; Verschueren, A.R.; Dekker, C. Room-temperature transistor based on a single carbon nanotube. *Nature* **1998**, *393*, 49–52. [[CrossRef](#)]
39. Valentini, L.; Armentano, I.; Kenny, J.; Cantalini, C.; Lozzi, L.; Santucci, S. Sensors for sub-ppm NO₂ gas detection based on carbon nanotube thin films. *Appl. Phys. Lett.* **2003**, *82*, 961–963. [[CrossRef](#)]
40. Kumar, D.; Chaturvedi, P.; Saho, P.; Jha, P.; Chouksey, A.; Lal, M.; Rawat, J.S.B.S.; Tandon, R.P.; Chaudhury, P.K. Effect of single wall carbon nanotube networks on gas sensor response and detection limit. *Sensor. Actuat. B Chem.* **2017**, *240*, 1134–1140. [[CrossRef](#)]
41. Ghodrati, M.; Farmani, A.; Mir, A. Nanoscale sensor-based tunneling carbon nanotube transistor for toxic gases detection: A first-principle study. *IEEE Sens. J.* **2019**, *19*, 7373–7377. [[CrossRef](#)]
42. Badhulika, S.; Myung, N.V.; Mulchandani, A. Conducting polymer coated single-walled carbon nanotube gas sensors for the detection of volatile organic compounds. *Talanta* **2014**, *123*, 109–114. [[CrossRef](#)]
43. Brahim, S.; Colbern, S.; Gump, R.; Moser, A.; Grigorian, L. Carbon nanotube-based ethanol sensors. *ACS Sym. Ser.* **2009**, *20*, 235502. [[CrossRef](#)] [[PubMed](#)]
44. Young, S.; Lin, Z. Ethanol gas sensors based on multi-wall carbon nanotubes on oxidized Si substrate. *Microsyst. Technol.* **2018**, *24*, 55–58. [[CrossRef](#)]
45. Leghrib, R.; Pavelko, R.; Felten, A.; Vasiliev, A.; Cané, C.; Gràcia, I.; Pireaux, J.-J.; Llobet, E. Gas sensors based on multiwall carbon nanotubes decorated with tin oxide nanoclusters. *Sensor. Actuat. B Chem* **2010**, *145*, 411–416. [[CrossRef](#)]
46. Villalpando-Páez, F.; Romero, A.; Muñoz-Sandoval, E.; Martínez, L.; Terrones, H.; Terrones, M. Fabrication of vapor and gas sensors using films of aligned CN_x nanotubes. *Chem. Phys. Lett.* **2004**, *386*, 137–143. [[CrossRef](#)]
47. Chang, Q.; Zhao, K.; Chen, X.; Li, M.; Liu, J. Preparation of gold/polyaniline/multiwall carbon nanotube nanocomposites and application in ammonia gas detection. *J. Mater. Sci.* **2008**, *43*, 5861–5866. [[CrossRef](#)]
48. Slobodian, P.; Riha, P.; Lengálová, A.; Svoboda, P.; Sába, P. Multi-wall carbon nanotube networks as potential resistive gas sensors for organic vapor detection. *Carbon* **2011**, *49*, 2499–2507. [[CrossRef](#)]
49. Sattari, S.; Reyhani, A.; Khanlari, M.; Khabazian, M.; Heydari, H. Synthesis of polyaniline–multi walled carbon nanotubes composite on the glass and silicon substrates and methane gas sensing behavior of them at room temperature. *J. Ind. Eng. Chem.* **2014**, *20*, 1761–1764. [[CrossRef](#)]

50. Zhao, J.; Buldum, A.; Han, J.; Lu, J.P. Gas molecule adsorption in carbon nanotubes and nanotube bundles. *Nanotechnology* **2002**, *13*, 195. [[CrossRef](#)]
51. Woods, L.; Bădescu, Ș.; Reinecke, T. Adsorption of simple benzene derivatives on carbon nanotubes. *Phys. Rev. B* **2007**, *75*, 155415. [[CrossRef](#)]
52. Dilonardo, E.; Penza, M.; Alvisi, M.; Di Franco, C.; Rossi, R.; Palmisano, F.; Torsi, L.; Cioffi, N. Electrophoretic deposition of Au NPs on MWCNT-based gas sensor for tailored gas detection with enhanced sensing properties. *Sensor. Actuat. B Chem.* **2016**, *223*, 417–428. [[CrossRef](#)]
53. Peng, S.; Cho, K. Ab initio study of doped carbon nanotube sensors. *Nano Lett.* **2003**, *3*, 513–517. [[CrossRef](#)]
54. Cella, L.N.; Chen, W.; Myung, N.V.; Mulchandani, A. Single-walled carbon nanotube-based chemiresistive affinity biosensors for small molecules: Ultrasensitive glucose detection. *J. Am. Chem. Soc.* **2010**, *132*, 5024–5026. [[CrossRef](#)] [[PubMed](#)]
55. Joshi, S.; Bhatt, V.D.; Wu, H.; Becherer, M.; Lugli, P. Flexible lactate and glucose sensors using electrolyte-gated carbon nanotube field effect transistor for non-invasive real-time monitoring. *IEEE Sens. J.* **2017**, *17*, 4315–4321. [[CrossRef](#)]
56. Pomowski, A.; Baricham, C.; Rapp, B.E.; Matern, A.; Laenge, K. Acoustic biosensors coated with phosphorylcholine groups for label-free detection of human C-reactive protein in serum. *IEEE Sens. J.* **2015**, *15*, 4388–4392. [[CrossRef](#)]
57. Raina, M.; Sharma, R.; Deacon, S.E.; Tiede, C.; Tomlinson, D.; Davies, A.G.; McPherson, M.J.; Waelti, C. Antibody mimetic receptor proteins for label-free biosensors. *Analyst* **2015**, *140*, 803–810. [[CrossRef](#)]
58. Ly, S.Y.; Cho, N.S. Diagnosis of human hepatitis B virus in non-treated blood by the bovine IgG DNA-linked carbon nanotube biosensor. *J. Clin. Virol.* **2009**, *44*, 43–47. [[CrossRef](#)]
59. Shao, K.; Zhang, C.; Ye, S.; Cai, K.; Wu, L.; Wang, B.; Zou, C.; Lu, Z.; Han, H. Near-infrared electrochemiluminescence biosensor for high sensitive detection of porcine reproductive and respiratory syndrome virus based on cyclodextrin-grafted porous Au/PtAu nanotube. *Sensor. Actuat. B Chem.* **2017**, *240*, 586–594. [[CrossRef](#)]
60. Wasik, D.; Mulchandani, A.; Yates, M.V. A heparin-functionalized carbon nanotube-based affinity biosensor for dengue virus. *Biosens. Bioelectron.* **2017**, *91*, 811–816. [[CrossRef](#)]
61. Boussaad, S.; Tao, N.J.; Zhang, R.; Hopson, T.; Nagahara, L.A. In situ detection of cytochrome c adsorption with single walled carbon nanotube device. *Chem. Commun.* **2003**, 1502–1503. [[CrossRef](#)]
62. Chao, L.; Curreli, M.; Lin, H.; Bo, L.; Zhou, C. Complementary detection of prostate-specific antigen using In₂O₃ nanowires and carbon nanotubes. *J. Am. Chem. Soc.* **2005**, *127*, 12484–12485.
63. Wang, C.-W.; Pan, C.-Y.; Wu, H.-C.; Shih, P.-Y.; Tsai, C.-C.; Liao, K.-T.; Lu, L.-L.; Hsieh, W.-H.; Chen, C.-D.; Chen, Y.-T. In situ detection of chromogranin a released from living neurons with a single-walled carbon-nanotube field-effect transistor. *Small* **2007**, *3*, 1350–1355. [[CrossRef](#)] [[PubMed](#)]
64. Filipiak, M.S.; Rother, M.; Andoy, N.M.; Knudsen, A.C.; Grimm, S.; Bachran, C.; Swee, L.K.; Zaumseil, J.; Tarasov, A. Highly sensitive, selective and label-free protein detection in physiological solutions using carbon nanotube transistors with nanobody receptors. *Sensor. Actuat. B Chem.* **2018**, *255*, 1507–1516. [[CrossRef](#)]
65. Cheng, H.; Jin, W.; Huang, X.; Liu, X.; Wang, F.; Guo, X.; Wu, Y.; Ying, Y.; Wen, Y.; Yang, H. A flexible carbon nanotube-modified poly(styrene-butadiene)-based dopamine sensor. *ACS Sym. Ser.* **2019**, *31*, 015505. [[CrossRef](#)]
66. Cheng, J.; Wang, X.; Nie, T.; Yin, L.; Wang, S.; Zhao, Y.; Wu, H.; Mei, H. A novel electrochemical sensing platform for detection of dopamine based on gold nanobipyramid/multi-walled carbon nanotube hybrids. *Anal. Bioanal. Chem.* **2020**, *412*, 2433–2441. [[CrossRef](#)]
67. Huang, Q.; Lin, X.; Tong, L.; Tong, Q.-X. Graphene quantum dots/multiwalled carbon nanotubes composite-based electrochemical sensor for detecting dopamine release from living cells. *ACS Sustain. Chem. Eng.* **2020**, *8*, 1644–1650. [[CrossRef](#)]
68. Dias, A.C.M.; Gomes-Filho, S.L.; Silva, M.M.; Dutra, R.F. A sensor tip based on carbon nanotube-ink printed electrode for the dengue virus NS1 protein. *Biosens. Bioelectron.* **2013**, *44*, 216–221. [[CrossRef](#)]
69. Sardesai, N.P.; Barron, J.C.; Rusling, J.F. Carbon nanotube microwell array for sensitive electrochemiluminescent detection of cancer biomarker proteins. *Anal. Chem.* **2011**, *83*, 6698–6703. [[CrossRef](#)]
70. Ahn, J.-H.; Kim, J.-H.; Reuel, N.F.; Barone, P.W.; Boghossian, A.A.; Zhang, J.; Yoon, H.; Chang, A.C.; Hilmer, A.J.; Strano, M.S. Label-free, single protein detection on a near-infrared fluorescent single-walled carbon nanotube/protein microarray fabricated by cell-free synthesis. *Nano Lett.* **2011**, *11*, 2743–2752. [[CrossRef](#)]
71. Kojima, A.; Hyon, C.K.; Kamimura, T.; Maeda, M.; Matsumoto, K. Protein sensor using carbon nanotube field effect transistor. *JPN J. Appl. Phys.* **2005**, *44*, 1596–1598. [[CrossRef](#)]
72. Williams, R.M.; Lee, C.; Heller, D.A. A fluorescent carbon nanotube sensor detects the metastatic prostate cancer biomarker uPA. *ACS Sensors* **2018**, *3*, 1838–1845. [[CrossRef](#)] [[PubMed](#)]
73. Villamizar, R.A.; Maroto, A.; Rius, F.X.; Inza, I.; Figueras, M.J. Fast detection of Salmonella Infantis with carbon nanotube field effect transistors. *Biosens. Bioelectron.* **2008**, *24*, 279–283. [[CrossRef](#)] [[PubMed](#)]
74. So, H.M.; Park, D.W.; Jeon, E.K.; Kim, Y.H.; Kim, B.S.; Lee, C.K.; Choi, S.Y.; Kim, S.C.; Chang, H.; Lee, J.O. Detection and titer estimation of Escherichia coli using aptamer-functionalized single-walled carbon-nanotube field-effect transistors. *Small* **2008**, *4*, 197–201. [[CrossRef](#)]
75. Kim, J.P.; Lee, B.Y.; Lee, J.; Hong, S.; Sim, S.J. Enhancement of sensitivity and specificity by surface modification of carbon nanotubes in diagnosis of prostate cancer based on carbon nanotube field effect transistors. *Biosens. Bioelectron.* **2009**, *24*, 3372–3378. [[CrossRef](#)]

76. Martínez, M.T.; Tseng, Y.-C.; Ormategui, N.; Loinaz, I.; Eritja, R.; Bokor, J. Label-free DNA biosensors based on functionalized carbon nanotube field effect transistors. *Nano Lett.* **2009**, *9*, 530–536. [[CrossRef](#)]
77. Sorgenfrei, S.; Chiu, C.-Y.; Gonzalez, R.L., Jr.; Yu, Y.-J.; Kim, P.; Nuckolls, C.; Shepard, K.L. Label-free single-molecule detection of DNA-hybridization kinetics with a carbon nanotube field-effect transistor. *Nat. Nanotechnol.* **2011**, *6*, 126–132. [[CrossRef](#)]
78. Ramnani, P.; Gao, Y.; Ozsoz, M.; Mulchandani, A. Electronic detection of microRNA at attomolar level with high specificity. *Anal. Chem.* **2013**, *85*, 8061–8064. [[CrossRef](#)]
79. Kurkina, T.; Vlandas, A.; Ahmad, A.; Kern, K.; Balasubramanian, K. Label-free detection of few copies of DNA with carbon nanotube impedance biosensors. *Angewandte Chem. Int. Ed.* **2011**, *50*, 3710–3714. [[CrossRef](#)]
80. Stine, R.; Robinson, J.T.; Sheehan, P.E.; Tamanaha, C.R. Real-time DNA detection using reduced graphene oxide field effect transistors. *Adv. Mater.* **2010**, *22*, 5297–5300. [[CrossRef](#)]
81. Cai, B.; Wang, S.; Huang, L.; Ning, Y.; Zhang, Z.; Zhang, G.-J. Ultrasensitive label-free detection of PNA-DNA hybridization by reduced graphene oxide field-effect transistor biosensor. *ACS Nano* **2014**, *8*, 2632–2638. [[CrossRef](#)] [[PubMed](#)]
82. Wang, S.; Li, L.; Jin, H.; Yang, T.; Bao, W.; Huang, S.; Wang, J. Electrochemical detection of hepatitis B and papilloma virus DNAs using SWCNT array coated with gold nanoparticles. *Biosens. Bioelectr.* **2013**, *41*, 205–210. [[CrossRef](#)] [[PubMed](#)]
83. Yin, Z.; He, Q.; Huang, X.; Zhang, J.; Wu, S.; Chen, P.; Lu, G.; Chen, P.; Zhang, Q.; Yan, Q.; et al. Real-time DNA detection using Pt nanoparticle-decorated reduced graphene oxide field-effect transistors. *Nanoscale* **2012**, *4*, 293–297. [[CrossRef](#)] [[PubMed](#)]
84. Tam, P.D.; Van Hieu, N.; Chien, N.D.; Le, A.-T.; Tuan, M.A. DNA sensor development based on multi-wall carbon nanotubes for label-free influenza virus (type A) detection. *J. Immun. Methods* **2009**, *350*, 118–124. [[CrossRef](#)] [[PubMed](#)]
85. Zribi, B.; Roy, E.; Pallandre, A.; Chebil, S.; Koubaa, M.; Mejr, N.; Magdinier Gomez, H.; Sola, C.; Korri-Youssoufi, H.; Haghiri-Gosnet, A.-M. A microfluidic electrochemical biosensor based on multiwall carbon nanotube/ferrocene for genomic DNA detection of Mycobacterium tuberculosis in clinical isolates. *Biomicrofluidics*. **2016**, *10*, 014115. [[CrossRef](#)]
86. Qiu, W.; Xu, H.; Takalkar, S.; Gurung, A.S.; Liu, B.; Zheng, Y.; Guo, Z.; Baloda, M.; Baryeh, K.; Liu, G. Carbon nanotube-based lateral flow biosensor for sensitive and rapid detection of DNA sequence. *Biosens. Bioelectr.* **2015**, *64*, 367–372. [[CrossRef](#)]
87. Star, A.; Tu, E.; Niemann, J.; Gabriel, J.-C.P.; Joiner, C.S.; Valcke, C. Label-free detection of DNA hybridization using carbon nanotube network field-effect transistors. *Proc. Natl. Acad. Sci.* **2006**, *103*, 921–926. [[CrossRef](#)]
88. Dong, X.; Lau, C.M.; Lohani, A.; Mhaisalkar, S.G.; Kasim, J.; Shen, Z.; Ho, X.; Rogers, J.A.; Li, L.J. Electrical detection of femtomolar DNA via gold-nanoparticle enhancement in carbon-nanotube-network field-effect transistors. *Adv. Mater.* **2008**, *20*, 2389–2393. [[CrossRef](#)]
89. Maehashi, K.; Matsumoto, K.; Kerman, K.; Takamura, Y.; Tamiya, E. Ultrasensitive detection of DNA hybridization using carbon nanotube field-effect transistors. *JPN J. Appl. Phys.* **2004**, *43*, L1558. [[CrossRef](#)]
90. Zheng, C.; Huang, L.; Zhang, H.; Sun, Z.; Zhang, Z.; Zhang, G.-J. Fabrication of ultrasensitive field-effect transistor DNA biosensors by a directional transfer technique based on CVD-grown graphene. *ACS Appl. Mater. Inter.* **2015**, *7*, 16953–16959. [[CrossRef](#)]
91. Tran, T.L.; Nguyen, T.T.; Tran, T.T.H.; Chu, V.T.; Tran, Q.T.; Mai, A.T. Detection of influenza A virus using carbon nanotubes field effect transistor based DNA sensor. *Phys. E Low Dimens. Syst. Nanostr.* **2017**, *93*, 83–86. [[CrossRef](#)]
92. Dastagir, T.; Forzani, E.S.; Zhang, R.; Amlani, I.; Nagahara, L.A.; Tsui, R.; Tao, N. Electrical detection of hepatitis C virus RNA on single wall carbon nanotube-field effect transistors. *Analyst* **2007**, *132*, 738–740. [[CrossRef](#)] [[PubMed](#)]
93. Thu, V.V.; Tam, P.D.; Dung, P.T. Rapid and label-free detection of H5N1 virus using carbon nanotube network field effect transistor. *Curr. Appl. Phys.* **2013**, *13*, 1311–1315. [[CrossRef](#)]
94. Fatin, M.F.; Rahim Ruslinda, A.; Gopinath, S.C.B.; Arshad, M.K.M. High-performance interactive analysis of split aptamer and HIV-1 Tat on multiwall carbon nanotube-modified field-effect transistor. *Inter. J. Bio. Macromol.* **2019**, *125*, 414–422. [[CrossRef](#)]
95. Yeh, Y.-T.; Tang, Y.; Sebastian, A.; Dasgupta, A.; Perea-Lopez, N.; Albert, I.; Lu, H.; Terrones, M.; Zheng, S.-Y. Tunable and label-free virus enrichment for ultrasensitive virus detection using carbon nanotube arrays. *Sci. Adv.* **2016**, *2*, e1601026. [[CrossRef](#)]
96. Lee, D.; Chander, Y.; Goyal, S.M.; Cui, T. Carbon nanotube electric immunoassay for the detection of swine influenza virus H1N1. *Biosens. Bioelectr.* **2011**, *26*, 3482–3487. [[CrossRef](#)]
97. Mandal, H.S.; Su, Z.; Ward, A.; Tang, X.S. Carbon nanotube thin film biosensors for sensitive and reproducible whole virus detection. *Theranostics* **2012**, *2*, 251–257. [[CrossRef](#)]
98. Silva, M.M.; Dias, A.C.; Silva, B.V.; Gomes-Filho, S.L.; Kubota, L.T.; Goulart, M.O.; Dutra, R.F. Electrochemical detection of dengue virus NS1 protein with a poly (allylamine)/carbon nanotube layered immunoelectrode. *J. Chem. Technol. Biotechnol.* **2015**, *90*, 194–200. [[CrossRef](#)]
99. Cabral, D.G.; Lima, E.C.; Moura, P.; Dutra, R.F. A label-free electrochemical immunosensor for hepatitis B based on hyaluronic acid-carbon nanotube hybrid film. *Talanta* **2016**, *148*, 209–215. [[CrossRef](#)]
100. Pinals, R.L.; Ledesma, F.; Yang, D.; Navarro, N.; Jeong, S.; Pak, J.E.; Kuo, L.; Chuang, Y.-C.; Cheng, Y.-W.; Sun, H.-Y. Rapid SARS-CoV-2 Detection by Carbon Nanotube-Based Near-Infrared Nanosensors. *medRxiv* **2020**. [[CrossRef](#)]
101. Gopinath, P.G.; Anitha, V.R.; Mastani, S.A. Design of biosensor array with current boost and signal conditioning circuits for HPV detection. *Alexa. Eng. J.* **2018**, *57*, 671–681. [[CrossRef](#)]